An Adapted Coherent Flow Power Doppler Beamforming Scheme for Improved Sensitivity Towards Blood Signal Energy

Kathryn Ozgun, Jaime Tierney, and Brett Byram

Department of Biomedical Engineering, Vanderbilt University, Nashville, TN, USA

kathryn.a.ozgun@vanderbilt.edu

Abstract—Ultrasonic flow imaging remains susceptible to cluttered imaging environments, which often results in degraded image quality. Coherent Flow Power Doppler (CFPD) is a beamforming technique that has demonstrated efficacy in mitigating the presence of diffuse clutter in flow images. CFPD depicts the normalized aperture domain coherence of the backscattered echo, which is described by the van Cittert-Zernike theorem. However, the use of a normalized coherence metric uncouples the image intensity from the underlying blood signal energy. As a result, CFPD is not a robust approach to study gradation in blood signal energy, which depicts the fractional moving blood volume. We have developed a modified beamforming scheme, termed power-preserving Coherent Flow Power Doppler (ppCFPD), which depicts a measure of mutual intensity, rather than normalized coherence. This approach retains the clutter suppression capability of CFPD, while preserving sensitivity toward the underlying signal energy, similar to conventional power Doppler. Efficacy of this approach was shown via Field II simulations, and in vivo feasibility was demonstrated in a human liver. Overall, this adapted approach shows promise as an alternative technique to depict flow gradation in cluttered imaging environments.

Index Terms—Ultrasound, Coherence, Blood Flow Imaging

I. INTRODUCTION

Achieving adequate sensitivity toward blood flow remains a substantial clinical challenge for ultrasonic imaging, particularly among overweight and obese patient populations [1]. Perception of blood flow is often obscured by insufficient suppression of thermal noise and acoustic clutter, which pertains to extraneous signals imposed by off-axis scattering, reverberation, and sound speed variation.

In prior literature, numerous techniques have been proposed to mitigate clutter on the basis of temporal and aperture-domain characteristics [2]–[5]. Among these are coherence-based beamformers, which exploit the predictable character of an incoherent source measured across an aperture. Mallart and Fink observed that the coherence of a backscattered echo is described by the van Cittert-Zernike (VCZ) theorem, and therefore may be written as a function of the transmitter aperture function and the reflectivity of the insonified medium [6]. In practice, this concept has been realized through calculations of inter-element RF signal coherence and adaptive beamsum weighting [7], [8].

Li and Dahl demonstrated that the use of a normalized coherence metric, previously employed in short lag spatial coherence (SLSC) imaging, improved sensitivity toward blood flow in comparison to conventional power Doppler (PD). This technique, termed Coherent Flow Power Doppler (CFPD), has shown efficacy in improving SNR and mitigating diffuse clutter sources [9]. However, a drawback of the CFPD technique is that the normalized coherence metric incurs a non-linear response toward signal power [1]. As investigated by Bottenus and Trahey, normalization causes the coherence metric to be sensitive to changes in noise power, which directly affects contrast and other metrics [10]. Additionally, normalization removes the relative signal energy from the image intensity, which compromises sensitivity toward flow gradation [1].

We propose a modified scheme, termed power-preserving Coherent Flow Power Doppler (ppCFPD). The objective of this work is to demonstrate that a modest modification to the CFPD beamforming scheme preserves the underlying blood signal intensity, while maintaining superior rejection of clutter and noise in comparison to conventional power Doppler.

II. PROPOSED BEAMFORMING SCHEME

For an aperture composed of N elements, the time-delayed received echo may be described as $y_i(n)$, where n indicates the sample through depth and i denotes the receive element. A slow-time filter is applied to the delayed channel data to suppress clutter that is approximately stationary. This isolates the blood signal from slowly-moving tissue; however, remaining acoustic clutter and noise may prevent adequate perception of blood flow.

To address the residual clutter and noise, the conventional CFPD technique subsequently measures the normalized coherence of the delayed channel data for an ensemble of M successive lags. However, normalization removes the relative strength of the received echo signals, which encodes the blood signal energy. Omission of the denominator in the calculation of normalized coherence yields the mutual intensity.

For a given lag, m, the mutual intensity may be written

$$\check{R}(m) = \frac{1}{N-m} \sum_{i=1}^{N-m} \sum_{n=n_1}^{n_2} y_i(n) y_{i+m}(n).$$
(1)

which is calculated for all pairs of time-delayed channel signals, y_i and y_{i+m} , separated by lag m. To reduce random errors, fast-time averaging over a kernel, described by n, spanning approximately one wavelength is employed.

The aperture domain coherence metric is defined as the summation of the mutual intensity for an ensemble of M successive lags, described in (2). After computing the aperture domain coherence metric for each pixel, the ppCFPD image is reconstructed via summation over a temporal ensemble of size A, shown below in (3). This summation effectively yields intensity with the units of amplitude squared. As a result, the amplitude of the ppCFPD image exhibits a power scale similar to power Doppler.

$$\check{V}(a) = \sum_{m=1}^{M} \check{R}(m) \tag{2}$$

$$ppCFPD = \sum_{a=1}^{A} \breve{V}(a)$$
 (3)

In comparison to normalized coherence, the mutual intensity expresses the co-variation of the signals. However, an assessment of the VCZ theorem yields that the mutual intensity observed between two signals, $P(x_1, f)$ and $P(x_2, f)$, takes a predictable form. Under assumption of the far field approximation, this may be written

$$R_p(x_1, x_2, z, f) = P(x_1, f)P(x_2, f) = \frac{\chi(f)}{z^4}R_o(x_1 - x_2).$$
(4)

where $\chi(f)$ is the scattering function and R_o is the autocorrelation of the transmit aperture function. The scattering function is governed by the insonified media, and in the context of flow, is a surrogate parameter for the fractional moving blood volume, as described by Rubin [11]. The autocorrelation of the transmit aperture function may be described as a function of lag. Fully developed speckle takes the form of a triangular function in the case of an unapodized linear array transducer, with a decreasing slope proportional to $\frac{m}{N}$ [6].

Therefore, the mutual intensity observed between two signals may be regarded as a function of the underlying signal amplitude and the separation between elements. For a given pixel, the blood signal retains the predictable triangular form employed in CFPD, with the magnitude uniformly scaled by the signal energy. Summing over an ensemble of lags delineates the blood signal from clutter, which exhibits limited aperture domain coherence.

III. DEPICTION OF BLOOD SIGNAL ENERGY

The expected nature of the beamformer can be generalized by observing the coherence between two delayed RF signals, denoted y_1 and y_2 . We begin with a description of the normalized coherence metric, which has been previously assessed [5]. Under the assumption that the delayed RF signals are real valued, the SLSC metric takes the form of Pearson's correlation coefficient, which may be symbolically written as

$$\rho(m) = \frac{\mathbb{E}[y_1 y_2] - \mathbb{E}[y_1] \mathbb{E}[y_2]}{\sqrt{(\mathbb{E}[y_1^2] - \mathbb{E}[y_1]^2)}} \sqrt{(\mathbb{E}[y_2^2] - \mathbb{E}[y_2]^2)}.$$
 (5)

The symbol \mathbb{E} denotes a mathematical expectation. To elaborate upon this expression, we assume the signal is composed of two zero-mean components: the signals of interest $(s_1$ and $s_2)$, and an additive clutter signal $(n_1$ and $n_2)$. The clutter noise is written as a white random noise variable and is uncorrelated from the signal of interest. As such, the above equation may be simplified to

$$\rho(m) = \frac{\mathbb{E}[(s_1 + n_1)(s_2 + n_2)]}{\sqrt{\mathbb{E}[s_1^2 + n_1^2]} \ \mathbb{E}[s_2^2 + n_2^2]}.$$
 (6)

Prior literature has drawn upon this equation, elucidating the associated relationship of the normalized coherence and signal power [5], [10]. As predicted by the VCZ theorem, the spatial covariance is proportional to a triangular function. Assuming the respective signal powers associated with any two elements on the array are approximately equal, we can portray the normalized coherence in terms of

$$\rho(m) = \frac{P_s(1 - \frac{n}{N})}{P_s + P_n} = \frac{1 - \frac{m}{N}}{1 + \frac{P_n}{P_s}},\tag{7}$$

where P_s represents the underlying blood signal power and P_n denotes noise power. Thus, the normalized coherence between two signals retains a dependence on the power of the noise signal.

In comparison, a similar expression can be written for the mutual intensity metric used in ppCFPD. Symbolically, this covariance may be written

$$\hat{\rho}(m) = \mathbb{E}[y_1 y_2] - \mathbb{E}[y_1] \mathbb{E}[y_2]. \tag{8}$$

Assuming that the same assumptions remain valid, we yield

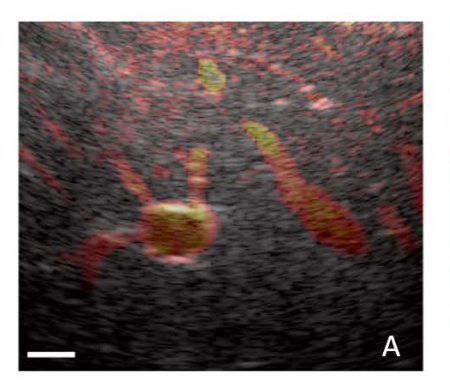
$$\hat{R}(m) = \mathbb{E}[(s_1 + n_1)(s_2 + n_2)] = P_s(1 - \frac{m}{N}) + P_n\delta(0).$$
 (9)

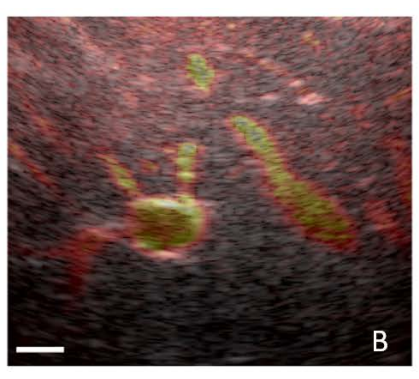
Therefore, we may theoretically obtain an estimate of the underlying blood signal power that is independent of additive noise by implementing a metric of covariance, excluding the zero-lag value.

IV. METHODS

A. Simulated Data Acquisition

For this investigation, simulated and *in vivo* flow data were obtained using steered plane waves. Simulated data was generated using Field II to study the performance of ppCFPD under varied conditions of clutter [12]. The simulated phantom included a single blood vessel with a 5mm diameter, embedded in a 9cm-by-5cm homogeneous tissue block at a 45° angle relative to the transducer. Laminar blood flow was simulated using scatterers moving in a parabolic flow pattern, with a maximum velocity of 5cm/sec. The simulated acquisitions were performed using a 128-element linear transducer with a center frequency of 3MHz and pitch of 0.257mm. For each acquisition, plane waves between -4° and 4° spaced





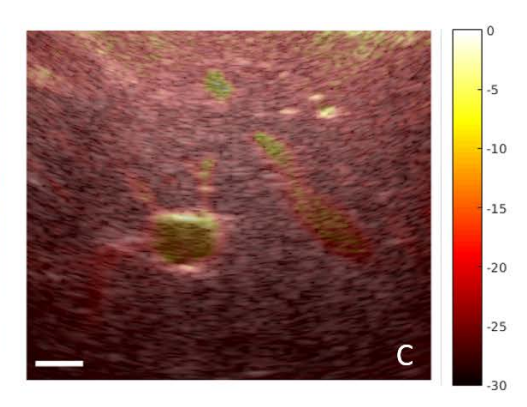


Fig. 1. Preliminary liver flow results overlaid on Bmode to demonstrate *in vivo* feasibility. Images produced via the ppCFPD algorithm (A) effectively delineated small vessels, which are nearly indistinguishable from the noise floor in the PD case (C). CFPD (B) improved sensitivity over PD, however, image intensity is not representative of the underlying signal energy. Scale bar represents 1cm.

by 1° were simulated at a PRF of 9KHz. The channel data was delayed using plane wave synthetic focusing (PWSF) as described by Montaldo et al., in which the delayed channel data acquired at consecutive angles were summed to produce a final PRF of 1KHz [13]. A 2Hz IIR filter cutoff was used for temporal clutter suppression.

B. In Vivo Data Acquisition

To further demonstrate the proposed algorithm, an *in vivo* example liver imaging case was obtained from a healthy adult male subject. Nine angled plane wave transmits spanning from -4° to 4°, spaced by 1°, were acquired using a C5-2 probe on a Verasonics research system (Verasonics Inc., Kirkland, WA). As performed for the simulated data cases, the channel data was delayed using PWSF, producing a final PRF of 600 Hz. Adapted demodulation was applied to suppress tissue motion, as described by Tierney [14]. A 30Hz IIR filter cutoff was used for temporal clutter suppression.

C. Image Quality Assessment

In order to evaluate the performance of the ppCFPD algorithm, we assessed image quality. Results were compared with PD and CFPD images generated from the same data. The image quality metrics included contrast, contrast-to-noise ratio (CNR), and root-mean-square signal-to-noise (SNRrms) calculations, measured as

$$Contrast = 10log_{10}(\frac{\bar{S}_i}{\bar{S}_c}), \tag{10}$$

$$CNR = \frac{|\bar{S}_i - \bar{S}_o|}{\sqrt{\sigma_i^2 + \sigma_o^2}},\tag{11}$$

$$SNR = 10log_{10}\left(\frac{\sqrt{\frac{1}{N}\sum_{i=1}^{N}S_{i}^{2}(i)}}{\sqrt{\frac{1}{M}\sum_{i=1}^{M}S_{o}^{2}(i)}}\right).$$
(12)

Negative pixel values may be produced in ppCFPD image formation due to partial and out-of-phase correlations. These values, associated with noise, are detrimental to image quality and inhibit log compression; thus, we set negative pixels to zero when displaying images and calculating image quality metrics, which is consistent with prior literature [15].

Preservation of blood signal energy was evaluated in terms of the capacity to resolve the fractional moving blood volume, in accord with a prior power Doppler assessment by Rubin et al. [11]. The intensity of a power Doppler signal encodes the fraction of moving blood scatterers incurring a Doppler shift, which indicates relative vascularity. This was assessed by incrementally decreasing the fraction of moving blood scatterers, until nearly all blood scatterers remained stationary. Five independent simulations of blood and tissue were generated for each fractional step. Additionally, discrimination of fractional moving blood velocity was studied in the presence of added noise at six blood signal-to-noise levels.

V. RESULTS AND DISCUSSION

A. Fractional Blood Volume

The average signal amplitude of the blood was measured for each trial, for all fractional iterations and noise cases. Curves were generated by measuring the mean and standard deviation of the average amplitude across all five trials at each fractional iteration. The curves were normalized to the highest mean value for each noise case, as shown below in Fig. 2. As described by Rubin et al., the PD signal may be considered a first-order approximation of the relative fraction of moving blood within an insonified region of interest [11]. For high blood signal-to-noise cases, the PD images are an effective linear estimator of the fractional moving blood volume. However, at a -10dB blood signal-to-noise ratio, the power Doppler signal is overwhelmed by the noise signal, and becomes unable to effectively estimate the fractional moving blood volume. The CFPD images exhibit decreasing amplitude in relation to decreasing fractional moving blood volume, however, exhibits sensitivity to the noise magnitude. In comparison, ppCFPD remains an effective approximation of the fractional moving blood volume despite varied noise environments.

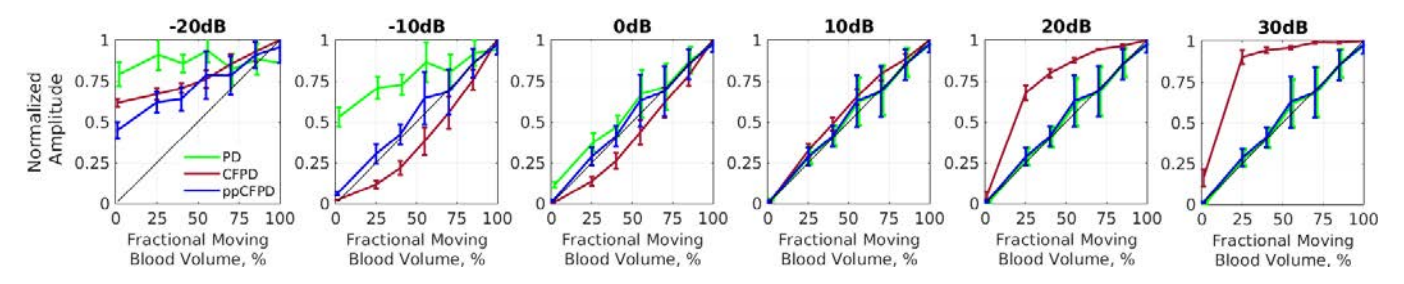


Fig. 2. The ppCFPD blood signal amplitude remains a linear approximation of the fractional moving blood volume despite variation in the blood signal-to-noise ratio from -20dB to 30dB. This may be observed in the figure, as the ppCFPD curve closely approximates the theoretical value, shown in black.

B. Image Quality

In matched simulations, ppCFPD yielded marked image quality improvement over PD, exhibiting contrast improvements up to 15.5dB, an increase in SNR up to 13.9dB and a CNR gain of 1.5. These improvements portray the greater sensitivity toward flow produced by ppCFPD, enabling the perception of flow in cluttered imaging environments. CFPD offers a slightly greater improvement in measured image quality, which is likely a result of squaring the SLSC metric prior to integration over the short-lag ensemble.

C. In Vivo Feasibility

Preliminary *in vivo* results are depicted in Fig. 1. As shown, CFPD and ppCFPD offered improved image quality over conventional PD. CFPD uncouples the pixel intensity from the underlying signal amplitude; however, the flow depicted in ppCFPD exhibits similar variation to the conventional PD, suggesting sensitivity to the blood signal energy is retained. Thermal imaging noise, which is likely to exhibit low or out-of-phase covariance, is effectively suppressed by the ppCFPD approach. Future study pertains to implementing a theoretical threshold to additionally mitigate low amplitude covariance associated with noise.

VI. CONCLUSIONS

We have theoretically described the anticipated nature of the ppCFPD beamforming technique, and its efficacy has been demonstrated through a preliminary investigation. The ppCFPD beamforming scheme mitigates diffuse clutter through the application of an aperture domain coherence measure, which improves the perception of vasculature in cluttered environments. The resultant image intensity portrays an approximation of the underlying blood signal energy, which addresses the primary drawback of employing a normalized coherence measure in conventional CFPD. Furthermore, the ppCFPD beamforming technique is robust to additive noise, which restricts the efficacy of conventional power Doppler. Overall, this approach shows promise for improving discrimination of blood flow within cluttered environments. Both CFPD and ppCFPD offer improved image quality over PD; however, we demonstrated that the CFPD technique exhibited non-linear characteristics as a function of varied SNR. In comparison, ppCFPD was robust to thermal noise power and retained sensitivity to variation in fractional moving blood

volume. This preliminary study suggests that a mutual intensity metric may be a valuable approach to assess blood flow gradation in cluttered imaging environments.

ACKNOWLEDGMENTS

The authors would like to thank the staff of the Vanderbilt University ACCRE computing resource. This work was supported by NIH-NIBIB award T32-EB021937 and NSF award IIS-1750994.

REFERENCES

- [1] J. Dahl et al., "Coherence beamforming and its applications to the difficult-to-image patient," *Proc IEEE Ultrason Symp*, pp. 1-10, 2017.
- [2] B. Byram, K. Dei, J. Tierney, D. Dumont, "A model and regularization scheme for ultrasonic beamforming clutter reduction," *IEEE Trans Ultrason Ferroelect Freq Control*, vol. 62, no. 11, pp. 1913-1927, 2015.
- [3] P. Song and S. Chen. "Spatiotemporal clutter filtering methods for in vivo microvessel imaging," *J Acoust Soc Am*, vol. 143, no. 3, pp. 1900-1900, 2018.
- [4] P. C. Li and M. L. Li, "Adaptive imaging using the generalized coherence factor," *IEEE Trans Ultrason Ferroelect Freq Contr*, vol. 50, no. 2, pp. 128-141, 2003.
- [5] N. Bottenus, B. C. Byram, J. J. Dahl and G. E. Trahey, "Synthetic aperture focusing for short-lag spatial coherence imaging," *IEEE Trans Ultrason Ferroelect Freq Contr*, vol. 60, no. 9, 2013.
- [6] M. Fink and R. Mallart, "The van Cittert-Zernike theorem in pulse echo measurements," J Acoust Soc Am, vol. 96, no. 5, 1991.
- [7] M. Lediju, G.E. Trahey, B.C. Byram, J.J. Dahl, "Short-lag spatial coherence of backscattered echoes: imaging characteristics," *IEEE Trans Ultrason Ferroelect Freq Contr*, vol. 58, no. 7, pp. 1377-1388, 2011.
- [8] K.W. Hollman, K.W. Rigby, M. O'Donnell, "Coherence factor of speckle from a multi-row probe," *Proc IEEE Ultrason Symp*, vol. 2, pp. 1257-1260, 1999.
- [9] Y. Li and J. Dahl, "Coherent flow power doppler (CFPD): flow detection using spatial coherence beamforming," *IEEE Trans Ultrason Ferroelect Freq Contr*, vol. 62, no. 6, pp. 1022-1035, 2015.
- [10] N. B. Bottenus and G. E. Trahey, "Equivalence of time and aperture domain additive noise in ultrasound coherence," *J Acoust Soc Am*, vol. 137, no. 1, 2015.
- [11] J. M. Rubin et al., "Fractional moving blood volume: estimation with power Doppler US.," *RSNA Radiology*, vol. 197, no. 1, 1995.
- [12] J. A. Jensen, "Field: A program for simulating ultrasound systems," 10th Nordic-Baltic Conf Biomed Imaging, vol. 4, no. 1, pp. 351-353, 1996.
- [13] G. Montaldo, M. Tanter, J. Bercoff, N. Benech and M. Fink, "Coherent plane-wave compounding for very high frame rate ultrasonography and transient elastography," *IEEE Trans Ultrason Ferroelect Freq Contr*, vol. 56, no. 3, pp. 489-506, 2009.
- [14] J. Tierney, C. Coolbaugh, T. Towse, and B. Byram, "Adaptive clutter demodulation for non-contrast ultrasound perfusion imaging," *IEEE Trans Med Imaging*, vol. 36, pp. 1979-1991, 2017.
- [15] A. Nair, T. Tran and M. L. Bell, "Robust short-lag spatial coherence imaging," *IEEE Trans Ultrason Ferroelect Freq Contr*, vol. 65, no. 3, pp. 366-377, 2018.